JOURNAL OF SCIENCE TECHNOLOGY AND EDUCATION 9(4), DECEMBER, 2021
ISSN: 2277-0011; Journal homepage: www.atbuftejoste.com

Performance Evaluation of Flow over Crump Weir Using Data-Driven Models

Sani Yakubu Khalifa, Babatunde Korode Adeogun, Abubakar Ismail, Morufu Ajibola Ajibike, Muhammad Mujahid Muhammad
Department of Water Resources and Environmental Engineering
Ahmadu Bello University Zaria, Kaduna state, Nigeria.

ABSTRACT
The flow characteristics changes with varying geometry of hydraulic weir and how the weir is inclined to the direction of flow in a channel. In this way, several studies have investigated the performance weirs experimental with paying much attention on the accurate prediction of discharge coefficient. Thus, the main objective of this study is to employ artificial intelligence (AI) techniques to predict discharge coefficient (C_d) of crump weir models. Hence, the precision and use of seven data-driven models including Bayesian neural network (BNN), multiple linear regression (MLR), multi-layer perceptron neural network (MLPNN), genetic algorithm (GA), support vector machine (SVM), Radial Basis Function (RBF) and curve fitting neural network (CFNN) were examined for estimating of the Cd. To achieve this, experiments were conducted on eighteen crump weir models of different apex angles 80^o, 90^o 100^o, 110^o 120^o and 130°. The upstream angles of the weir models were set in decreasing order of 85^o, 70^o, 55^o, 40^o, 25^o and 10^o. While the downstream angles were increased as 15^o, 20^o, 25^o, 30^o, 35^o and 40^o respectively. 360 laboratory test results were used, 70% for training, 15% for testing and 15% for validation. And statistical parameters of coefficient of determination (R^2), root-mean-square error (RMSE), mean absolute error (MAE), were employed as the criteria for the comparison of the models' performance. Results showed good agreements between the observed and estimated values using the AI-based models. However, among these models, the CFNN managed to estimate the Cd of the weir with the highest precision and accuracy than the rest of the models with ($RMSE=0.1635x10^{-4}$, $R^2=0.9981$,). Also, it was found that the most efficient crump was weir model 17 for having the least C_d of 1.14914 and least percentage error of 12.97412, which has been optimized using GA with C_d value of 1.14815.

ARTICLE INFO
Article History
Received: August, 2021
Received in revised form: August, 2021
Accepted: November, 2021
Published online: December, 2021

KEYWORDS
Crump Weir, Discharge Coefficient, Channel, Experiments, Artificial Intelligence

INTRODUCTION

The Crump section *flat-vee* weir is favored by hydrometrics because of the accuracy and range of flow measurement it exhibited. It is comparatively insensitive to submerged conditions and ease of determination of flow curves for any width, and its coefficient of discharges remain through undrown condition. However, this type of weir is disliked by fishermen because it can present a barrier to migration of fish (Rickard *et.al.*2003). As such it becomes necessary to investigate the behavior of the flow over the crump weir. In this way, few studies have been devoted to evaluating the flow over crump weirs, for example, Bos, 1989 was the first to study the flow characteristics of trapezoidal profile weirs systematically. He conducted a series of experiments on these types of weirs with both upstream and downstream side slopes. The discharge coefficient was determined for free flow conditions using different discharge values. Also, Al-Naely *et al.*, 2018 placed crump weirs in a channel as a control device in order to the flow

Corresponding author: Yakubu, S. K. ✉ *Khalees2k1@gmail.com* ✉ *Department of Water Resources and Environmental Engineering Ahmadu Bello University, Zaria.*

rate, a new performance for the crump weirs was observed as a result of adding an opening holes in the model of crump weir. The opening holes act as energy dissipaters and improvers for the discharge coefficient (C_d), where higher values of the discharge coefficient (C_d) were recorded in comparison with conventional weir under the same laboratory conditions. In the same vein, the creation of an opening in a broad-crested weir was found to increase the discharge coefficient and consequently improving the discharge (Daneshfaraz et al. 2019). Similarly, Khalifa & Umar, 2018 conducted experiments on crump weir models of different apex angles, they demonstrated that increase in the apex angle resulted in decrease in discharge coefficient. Hence, controlling the amount of discharge over different hydraulic structures was always a field of interest for researchers, with a view of decreasing sedimentation in reservoirs (Zahabi et al. 2018).

THEORETICAL BACKGROUND

Governing Equations

The discharge was estimated using the equation governing the modelling of flow over crump weir by determining the upstream flow head (h). Point gauge was used to measure the, h, above the crump weir (Arora, 2005). Thus, for modular flow over the crump weir, when the weir operates undrowned, the modular discharge is expressed as follows:

$$Q_m = C_d\sqrt{g}\,.\,bH_o^{\frac{3}{2}}. \qquad (1)$$

C_d and H_o can be determined using Equations (2) and (3) respectively

$$C_d = 1.163\left(1 - \frac{0.0003}{h}\right)^{1.5} \qquad (2)$$

$$H_o = y_o + \frac{V_o^2}{2g} \qquad (3)$$

Where, Q_m = Discharge for modular flow (m^3/s), C_d = Modular discharge coefficient, g = gravity (m^2/s), b = Breath of weir (m), H_o = Total head upstream of the weir crest (m), y_o = upstream water level (m), $\frac{V_o^2}{2g}$ = upstream velocity head (m).

However, for non-modular flow, when the weir operates drowned, a single measurement of upstream head is not sufficient to calculate the actual flow as the upstream head is affected by changes in the downstream head. In this case, a dimensionless reduction factor is introduced to correct the non-modular flow as given by Equation (4):

$$f = Q/Q_m \qquad (4)$$

Where, Q = Discharge for non-modular flow (m^3/s)

Artificial Neural Networks

Artificial neural network (ANN) is a nonlinear mathematical model that is able to simulate arbitrarily complex nonlinear processes, which relate inputs and outputs of any system. In many complex mathematical problems that lead to solving complex nonlinear equations, multilayer perceptron networks are common types of ANN widely used by researchers (Parsaie 2016; Moazamnia et al. 2019).

Support Vector Machines

Support vector machines operate based on data mining algorithms and are like other artificial intelligent methods. It was used in different fields of hydrology (e.g., Nadiri et al. 2017) and Hydraulics (e.g., Sadeghfam et al. 2019). Support vector machines are an efficient learning system based on the theory of optimization that uses the inductive principle of minimization of structural errors and lead to a general optimal response.

Multi-layer Perceptron Neural Network (MLPNN)

MLPNN is a computational method which tries to propose a mapping between input space (input layer) and optimal space (output layer) by understanding the inherent relationships among data with the help of learning process and using simple processors called neurons (Heidari *et al.*, 2016). The high speed of processing and flexibility in the face of unwanted errors are the features of this model. Its main advantage is its high speed and optimal precision in the prediction of complex variables with linear and non-linear mapping.

Multiple Linear Regression (MLR)

MLR is the most common regression which is employed to create a linear relationship between a dependent variable such as y and a set of independent variables such as $x\ x\ x_{1\,2\,3}, , , \ldots, x_n$ [J.P. Resop, 2006]. The linear equation of this method is in the form of Equation (3.10).

Corresponding author: Yakubu, S. K. ✉ *Khalees2k1@gmail.com* ✉ *Department of Water Resources and Environmental Engineering Ahmadu Bello University, Zaria.*

$y = +b_0 \quad b \quad x_1 \quad _1 \quad + \quad b \quad x_2 \quad _2 \quad +\ldots$ *(3.10)*

The performance and precision of regression methods highly depend on the sample size, and sample size can limit statistical models [Ghorbani et al, 2017].

Multilayer Perceptron (MLP)

Multilayer perceptron (MLP) network is the most commonly used neural network model applied in water engineering issues; for training, this network, a back-propagation learning algorithm which is a learning method with an observer, is used. The purpose of training a neural network is to arrange the network parameters (weights and biases) by providing training patterns, in a way that by representing the same patterns, the resulted error between the optimal response and network is minimized.

Mohammad Zounemat *et al.,* 2019 have examined the precision and use of six data driven models including BNN, MLR, MLPNN, GEP, LSSVM and CHAID for estimation of discharge passing triangular Arced labyrinth weir. MLPNN managed to estimate the discharge passing the weir with the highest precision (RMSE = 0.00385, R^2 = 0.999).

Reza Norouzi *et al.,* 2019 have investigated the performance of MLP, RBF and SVM in predicting the discharge coefficient (Cd) of lybrinth weirs. The performance of the MLP model was excellent with RMSE and R^2 of 0.019 and 0.985 respectively.

In the studies of Zounemat *et al.,* 2019, they applied various hybrid meta-heuristic MLPNN and ANFIS for predicting flow parameters of piano key weir flow.

METHODOLOGY

Fabrication of the Experimental Models

The experimental work was conducted on eighteen crump weir models of different apex angles of 80°, 90° 100°, 110° 120° and 130°. Accordingly, the upstream angles of the models were decreased to have the following values 85°, 70°, 55°, 40°, 25° and 10° , and to as well increasing the downstream angles as 15°, 20°, 25°, 30°, 35° and 40° respectively, which will sum up to give 180° as the total angles in a triangle as shown in Figure 1. Plywood of 22 mm thickness was used in fabricating the main body of the crump weirs.

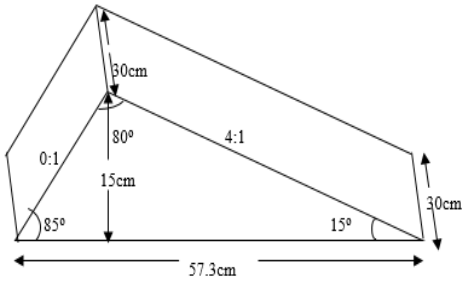

Figure 1: The schematic view of crump weir model 1 of apex angle 80°, upstream angle and slope, 85° and 0:1, downstream angle and slope, 15° and 4:1 respectively.

Table 1.0: Geometric Factors of Crump Weir Models

Model	Upstream Slope	Downstream Slope	Model width 'b' (cm)	Crest Height 'P' (cm)	Apex Angle (degree)	Upstream Angle(degree)	Downstream Angle(degree)
1	0.1:1	4:1	30	15	80	85	15
2	0.4:1	3:1	30	15	90	70	20
3	0.7:1	2:1	30	15	100	55	25
4	1:1	2:1	30	15	110	40	30
5	2:1	1:1	30	15	120	25	35
6	6:1	1:1	30	15	130	10	40

Corresponding author: Yakubu, S. K. ✉ *Khalees2k1@gmail.com* ✉ *Department of Water Resources and Environmental Engineering Ahmadu Bello University, Zaria.*

JOURNAL OF SCIENCE TECHNOLOGY AND EDUCATION 9(4), DECEMBER, 2021
ISSN: 2277-0011; Journal homepage: www.atbuftejoste.com

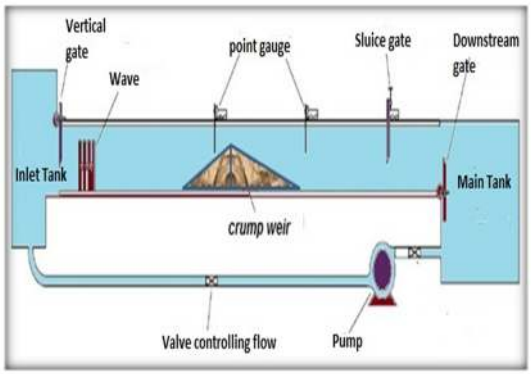

Figure 2: Sketch of Crump Weir Model and Experimental flume.

Experimental Procedure:

The crump weirs were installed in the flume with the help of sealants to prevent leakage, which has to be levelled. One vernier were located downstream the weir and the other upstream. The verniers were zeroed with the bed of the channel.

Seventy-two models were fabricated for which the angles were varied, 80°, 90°, 100°, 110°,120°, and 130° Experiment were then be ran for each model and various heads and their corresponding discharges were recorded; The procedure has five (5) runs. Each run has a different flow rate and a set of four (4) y_o and y_1 depths; two sets for modular flow condition and the other two sets for non-modular flow condition. The initial flow rate were set. Then, y_o and y_1 depths were recorded for the following conditions: Modular flow: without stop block (gate). Modular flow: one full stop block (gate) (y_1 should be the only depth that changes). Non-modular flow: Add a half of one stop block (gate). (y_1 and y_o depth that change). Non-modular flow: Add one quarter of a stop block (gate). The flow rate were increased at constant interval.

Modular Flow

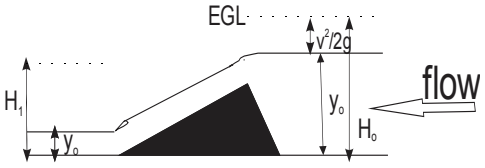

Figure 5: Crump weir during modular flow condition

Non-Modular Flow

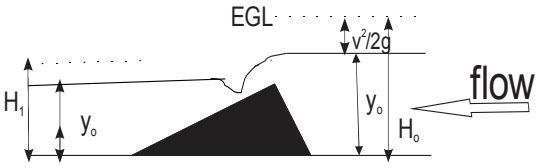

Figure 6: Crump weir during non-modular flow condition

Heights (P=10cm, 15cm, 20cm) were used as a crump weir models. For each type of crump three types of surface roughness were used. The first one were a smooth PVC, the second one is coated with a uniform sand D_{50} =0.72 mm (D_{50}=is the sieve diameter in which 50% of material are finer), while the third is covered by gravel of D_{50}= 3.6 mm. Eighteen models were used to conduct the experimental study. In each run the selected model were inserted along the width of the flume. Then the pump started at desired flow rate and after the flow stability were achieved the water surface level upstream and above the weir model were measured using point gauge. For each type of the crump weir a series of tests under different flow rates were conducted. The pump were activated and the discharge were adjusted using a control valve and the reading of the point gauge were recorded to give the head above crump weir required for the calculation of estimated discharge; At the beginning of each run the control valve were adjusted to alter the head; For each head recorded, the actual discharge were measured by direct method using the weighing arrangement provided at the tail end of the flume. The previous steps were repeated for each of the five runs of experiments to be conducted for each model. A total of 360 runs were conducted.

Determination of Observed Discharge (Q_o)

The observed discharge, Q_o, was measured experimentally using the gravimetrical method. Throughout the experiment, 100kg of water were collected by means of the weighing balance (see plate II) attached to the flume and stopwatch was used to obtain the time taken to collect the 100kg for onward determination of discharge.

Corresponding author: Yakubu, S. K. ✉ *Khalees2k1@gmail.com* ✉ *Department of Water Resources and Environmental Engineering Ahmadu Bello University, Zaria.*

Volume, V = mass/density
Observed discharge, Q_o = Volume / average time
Average time = $\frac{(t_1 + t_2)}{2}$ (5)

Determination of Estimated Discharge (Q_e)

The discharge equation for the crump weir was used to compute the estimated discharge using the flow heads. Point gauge will be used to measure the flow head (h) above the crump weir (Arora, 2005).

$$Q_m = C_d\sqrt{g}\,.\,bH_o^{\frac{3}{2}}. \quad (1)$$

$$C_d = 1.163\left(1 - \frac{0.0003}{h}\right)^{1.5} \quad (2)$$

$$H = y + \frac{V^2}{2g} \quad (3)$$

Derivation of Discharge Coefficient

In order to validate the suitability of the theoretical equations, the maximum of the absolute value of the deviation of the data from the model was obtained as:

$$\text{MaxErr} = \max\left(abs(C_{do} - C_{de})\right) \quad (7)$$

Where, C_{do} = Experimental Discharge Coefficient = Q_o / Q_e
C_{de} = Estimated Discharge Coefficient

$$Cd = (D_{50}, P, h, Q, \theta) \quad (8)$$

Thus, by dimensional analysis and using the approach of Buckingham's π-theorem, Equation (8) becomes:

$$Cd = f\left(\frac{D_{50}}{P}\theta, \frac{h}{P}\right) \quad (9)$$

It follows that Equation (9) can be expressed as Equation (10) based on dimensional homogeneity:

$$C_d = k_1\left[\frac{D_{50}\theta}{P}\right]^a + k_2\left[\frac{h}{P}\right]^b \quad (10)$$

Where, K_1, K_2, a, and b are parameters to be estimated by regression analysis.

RESULTS AND DISCUSSION

Computation of Discharge Coefficients (C_d)

Tables 2 show the values of C_d obtained from Equations 1 and 2 respectively. The head measurements were obtained by means of the point gauge.

Table 2: Discharge characteristics for model 1:

Q_o=V/t/m3/s	y_o/m	ho=yo - 0.10/m	y_1/m	H_O/m	H_1/m	Cd	Q_e/m³/s	% Error
0.001515	0.120	0.020	0.060	0.121	0.065	1.13693	0.00133	12.04391
0.001563	0.160	0.060	0.110	0.175	0.115	1.15429	0.00135	13.36654
0.001613	0.194	0.094	0.135	0.210	0.140	1.15744	0.00139	13.60220
0.001667	0.210	0.110	0.130	0.228	0.150	1.15825	0.00144	13.66252
0.001724	0.218	0.118	0.100	0.235	0.160	1.15857	0.00149	13.68652
Average						1.15310	0.001400	13.27234

Estimated discharge and C_d for PVC

Q_o=V/t/m3/s	y_o/m	ho=yo - 0.10/m	y_1/m	H_O/m	H_1/m	Cd	Q_e/m³/s	% Error
0.00150	0.125	0.025	0.060	0.130	0.060	1.14213	0.00131	12.44421
0.00158	0.167	0.067	0.100	0.177	0.110	1.15520	0.00136	13.43472
0.00164	0.193	0.093	0.120	0.208	0.140	1.15738	0.00142	13.59774
0.00170	0.208	0.108	0.060	0.227	0.150	1.15816	0.00146	13.65596
0.00175	0.215	0.115	0.060	0.232	0.150	1.15845	0.00151	13.67792
Average						1.15426	0.001412	13.36211

Table 3: Summary of models performance based on Cd and Percentage Error

Model Number	Cd Average	Percentage Error	Ranking
17	1.14914	12.97412	1
2	1.15189	13.17617	2
8	1.15122	13.18413	3

Corresponding author: Yakubu, S. K. ✉ *Khalees2k1@gmail.com* ✉ *Department of Water Resources and Environmental Engineering Ahmadu Bello University, Zaria.*

16	1.15223	13.20521	4
4	1.15313	13.27629	5
15	1.15383	13.32875	6
5	1.15406	13.34741	7
7	1.15414	13.35236	8
1	1.15425	13.36062	9
11	1.15425	13.36155	10
10	1.15433	13.36725	11
13	1.1544	13.37097	12
3	1.15449	13.37998	13
14	1.15476	13.39963	14
9	1.15483	13.40455	15
12	1.15527	13.43799	16
18	1.15546	13.4523	17
6	1.15553	13.45773	18

Table 4: Summary of the statistical analysis of Cd predicted by MLP using different neurons.

	Training		Validation		Testing	
No of neurons	MSEx(10^{-6})	R^2	MSEx(10^{-6})	R^2	MSEx(10^{-6})	R^2
1	9.0141	0.9123	7.5607	0.9152	4.5334	0.9613
2	5.0244	0.9392	5.8012	0.9301	23.735	0.8881
3	8.6095	0.9116	6.2662	0.9356	6.7934	0.9419
4	7.5581	0.9154	7.8690	0.9376	7.0532	0.9386
5	8.1319	0.9172	7.4021	0.9139	25.307	0.8497
6	7.7184	0.9283	6.2652	0.9111	7.1875	0.9115
7	1.9925	0.7902	2.4047	0.6565	17.668	0.8180
8	9.0060	0.8856	5.1653	0.7087	16.042	0.8045
9	8.1825	0.9234	7.0573	0.9161	1.8738	0.9821
10	8.1417	0.9251	4.6387	0.9309	6.2766	0.9290
11	1.0583	0.9090	3.7310	0.9579	7.0051	0.9331
12	4.3199	0.9458	2.1757	0.8691	7.2633	0.9435
13	7.8978	0.9175	6.1824	0.9432	6.5836	0.9363
14	9.4249	0.9035	8.5379	0.9214	6.3073	0.9325
15	4.7196	0.9475	4.2265	0.9404	23.272	0.8592
16	9.1488	0.9180	5.5131	0.8933	8.6496	0.9166
17	7.7760	0.9240	8.3009	0.9161	5.6503	0.9328
18	3.9774	0.9525	2.2298	0.8719	189.13	0.5615
19	8.3764	0.9227	7.4020	0.9137	0.9750	0.8849
20	1.0319	0.9037	6.4052	0.9190	7.6421	0.9132

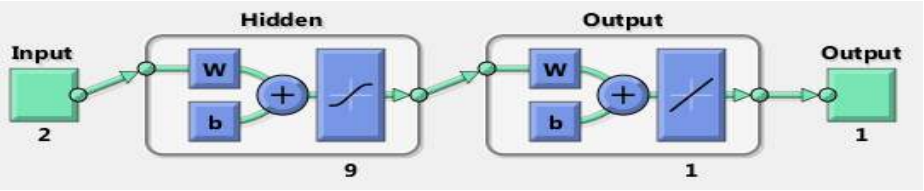

Figure 7: MLP Levenberg Marquardt Neural Network Diagram

Corresponding author: Yakubu, S. K. ✉ *Khalees2k1@gmail.com* ✉ *Department of Water Resources and Environmental Engineering Ahmadu Bello University, Zaria.*

JOURNAL OF SCIENCE TECHNOLOGY AND EDUCATION 9(4), DECEMBER, 2021
ISSN: 2277-0011; Journal homepage: www.atbuftejoste.com

DISCUSSION OF RESULT

Variation of Cd with (h/P)

The dimensional analysis for the variables affecting Cd value of weirs shows that the value (h/p) (Where h is head of the water on the weir, P height of the weir), has a greatest influence on Cd value. The calculated values of h/P are plotted against the Cd values for each weir and for each surface roughness's as shown in Figure 9. The figure shows that Cd value increase with increasing in h/P values for all the cases. Also it's evident from these figures that the gradient of the curve fit the points are decrease with increase in weir height, this means that the effect of h/P on Cd values will increase with increase in weir height.

Predicting the Cd of Crump Weir Using ANN

Results of evaluating the precision of the data-driven models in the estimation of Cd of crump weirs in the training and testing sets are presented in Tables 5 and 6 respectively. Comparison of the values provided in Table 6 shows that CFNN managed to estimate discharge passing the weir with the highest accuracy (RMSE= 0.1635×10^{-6} MAE=0.4713×10^{-3} R^2 =0.9981). Also, CFNN was followed by MLPNN, BNN, GA, MLR, RBF and SVM.

Eqs. (15) demonstrate the extracted relationships between independent and dependent variables in the CFNN model. Scatter plots presented in Figs. 14 and 15 show the results of BNN and MLPNN respectively indicating their good precision in estimating the performance of the crump weir.

In this study, the precision of seven data-driven models was evaluated for the estimation of Cd for crump weir. Final results showed that CFNN could estimate the discharge passing the weir with the highest precision. Also, due to the effect of input parameters of the model on the estimation accuracy, CFNN precision was evaluated using the various combination of the input parameters.2 different independent variables were used for constructing the applied models. In order to investigate the importance of each variable in the final performance of the models.

Table 7 shows the sensitivity analysis of Coefficient of discharge, Cd. The sensitivity analysis was carried, in order to evaluate the significance of input variables on the Coefficient of discharge. The sensitivity analysis was performed using the ANN model due to the high value of correlation coefficient and minimum error it produced. Consequently, the parameter ($\frac{h}{P}$) was found to be the most effective parameter with R =0.9971, MSE = 3.8513×10^{-4} on the prediction of Cd. While the function ($\frac{D_{50}\theta}{P}$) was found to be the least effective parameter on the prediction of Cd.

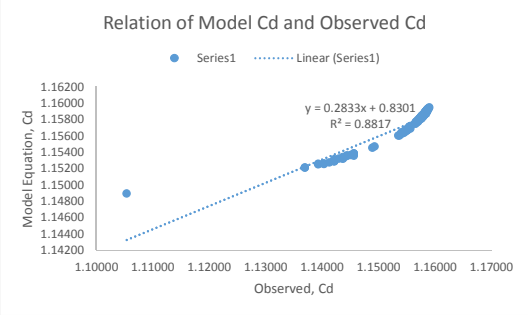

Figure 8: ANN verification of Cd from Model Equation

Table 5. Results of evaluating the performance of data driven models in the training phase.

Models	MSE ×(10^{-6})	MAE ×(10^{-3})	R^2
MLP	8.1825	0.9874	0.9234
BNN	7.9003	0.8452	0.9192
RBF	2897.6	1.7652	0.8400
SVM	4232.7	2.6745	0.7300

Table 6. Results of evaluating the performance of all the applied models in the testing phase.

Models	MSE ×(10^{-6})	MAE ×(10^{-3})	R^2
CFNN	0.1635	0.4713	0.9981
MLP	1.8738	0.6704	0.9821
BNN	3.4682	0.7461	0.9669

Corresponding author: Yakubu, S. K. ✉ *Khalees2k1@gmail.com* ✉ *Department of Water Resources and Environmental Engineering Ahmadu Bello University, Zaria.*

GA	3.9641	0.8452	0.9573
MLR	2611.7	1.4233	0.8700
RBF	2672.6	1.5712	0.8600
SVM	3288.7	2.1005	0.7900

Finally, the precision of the models in estimating the discharge passing the weir was evaluated using the root-mean square error (RMSE), mean absolute percentage error (MAE), R^2 (coefficient of determination). The best values of these criteria were 0, 0, and 1 respectively.

$$RMSE = \sqrt{\frac{1}{n}\sum_{j=1}^{n}(y_j - \hat{y}_j)^2} \quad (12)$$

$$MAE = \frac{1}{n}\sum_{j=1}^{n}|y_j - \hat{y}_j| \quad (13)$$

$$\hat{R}^2 = 1 - \frac{\sum_{i=1}^{n}(Y_i - \hat{Y}_i)^2}{\sum_{i=1}^{n}(Y_i - \bar{Y})^2} = 1 - \frac{\frac{1}{n}\sum_{i=1}^{n}(Y_i - \hat{Y}_i)^2}{\frac{1}{n}\sum_{i=1}^{n}(Y_i - \bar{Y})^2} \quad (14)$$

In Eqs. (12)–(14), y is the actual Cd, $\hat{y}$ is their saverage, n is the number of estimations.

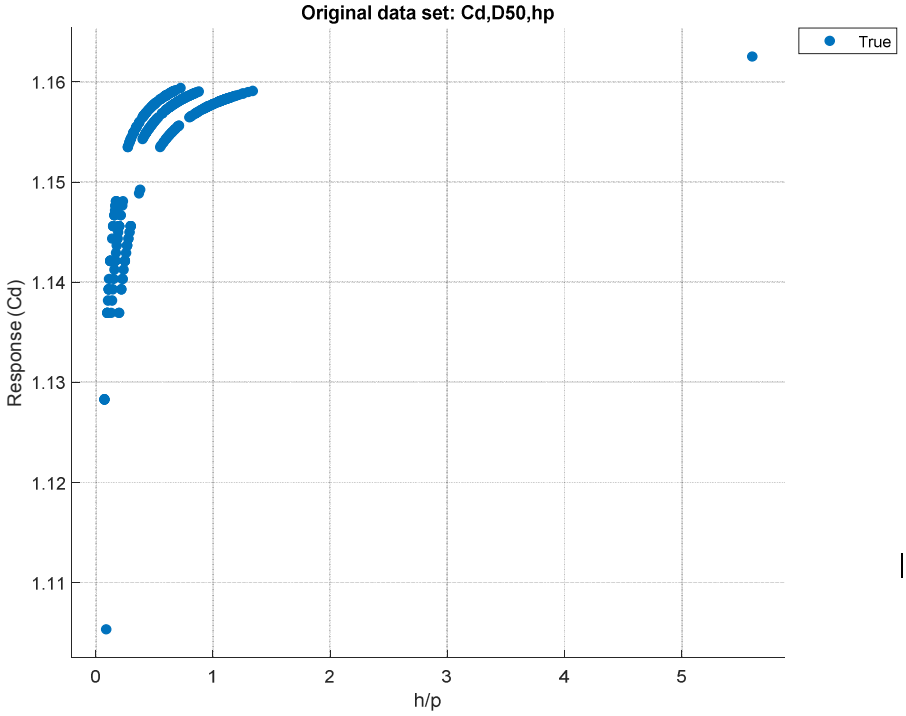

Figure 9: Relation of Cd and h/p using (MLR) model

Corresponding author: Yakubu, S. K. ✉ *Khalees2k1@gmail.com* ✉ *Department of Water Resources and Environmental Engineering Ahmadu Bello University, Zaria.*

JOURNAL OF SCIENCE TECHNOLOGY AND EDUCATION 9(4), DECEMBER, 2021
ISSN: 2277-0011; Journal homepage: www.atbuftejoste.com

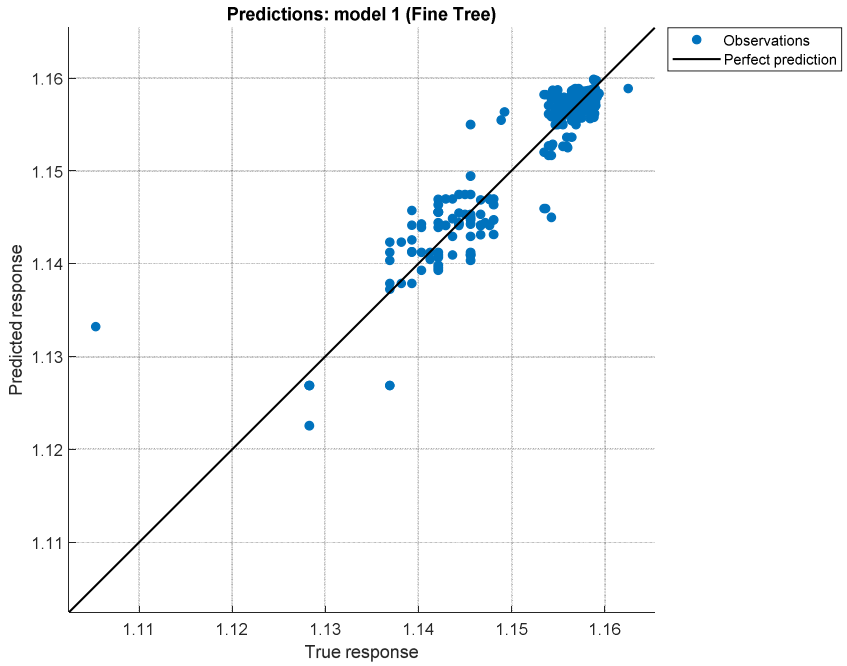

Figure 10: Relation of Cd predicted and Actual value using (MLR) model

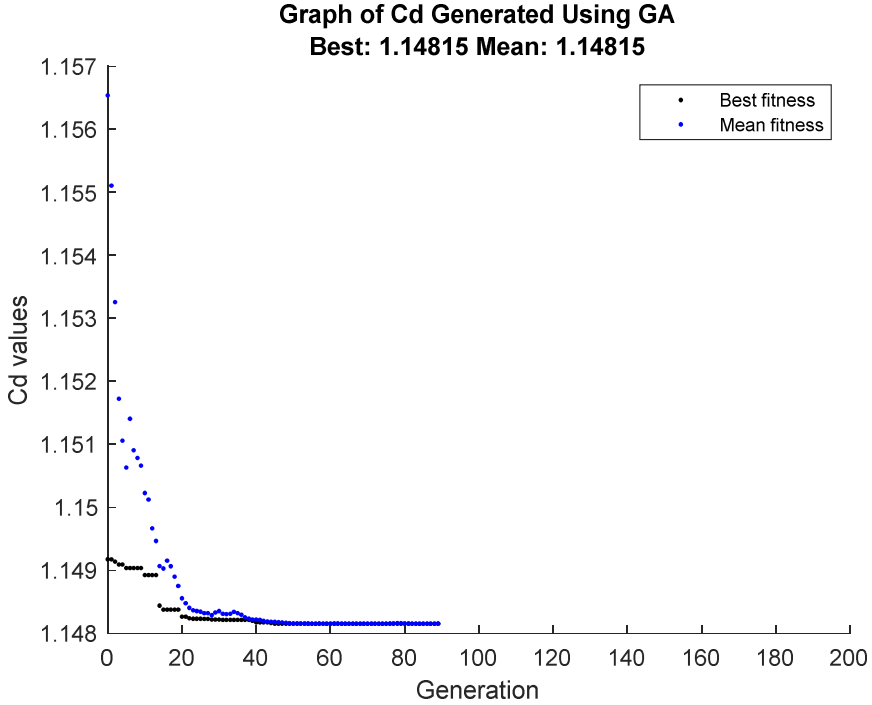

Figure 11: Relation of Cd generated using Genetic Algorithm (GA) model

Corresponding author: Yakubu, S. K. ✉ *Khalees2k1@gmail.com* ✉ *Department of Water Resources and Environmental Engineering Ahmadu Bello University, Zaria.*

JOURNAL OF SCIENCE TECHNOLOGY AND EDUCATION 9(4), DECEMBER, 2021
ISSN: 2277-0011; Journal homepage: www.atbuftejoste.com

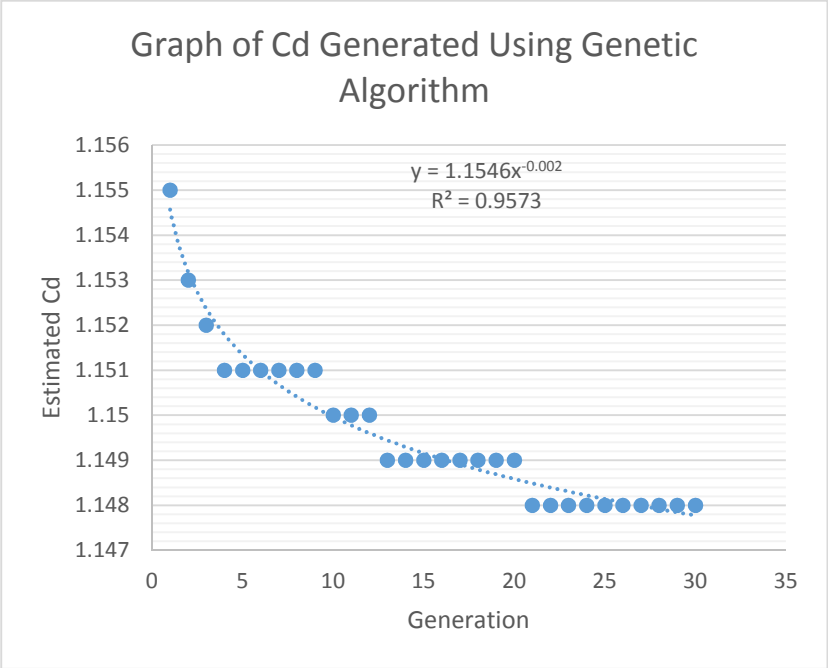

Figure 12: Relation of Cd Generated using Genetic Algorithm (GA) model

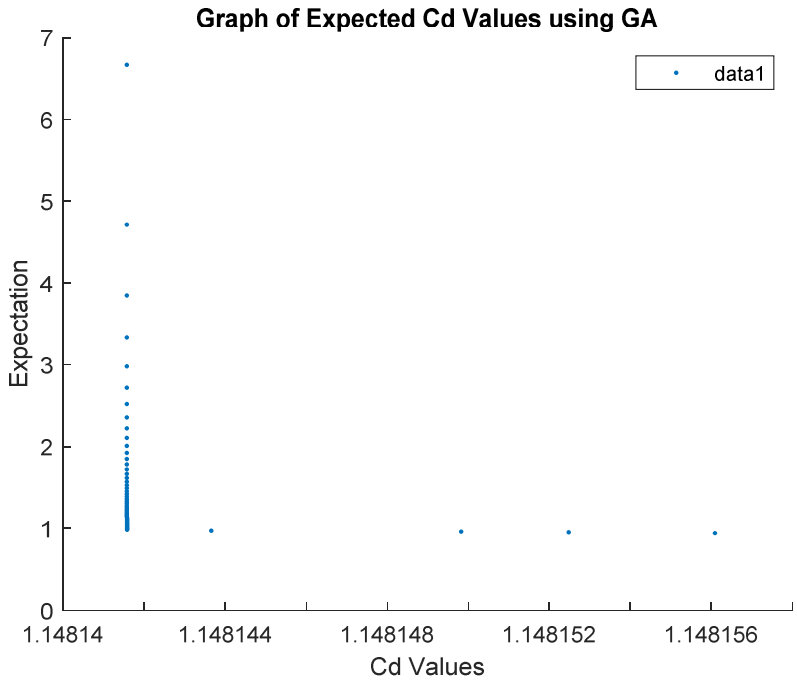

Figure 13: Relation of expected Cd fitness value using Genetic Algorithm (GA) model

Corresponding author: Yakubu, S. K. ✉ *Khalees2k1@gmail.com* ✉ *Department of Water Resources and Environmental Engineering Ahmadu Bello University, Zaria.*

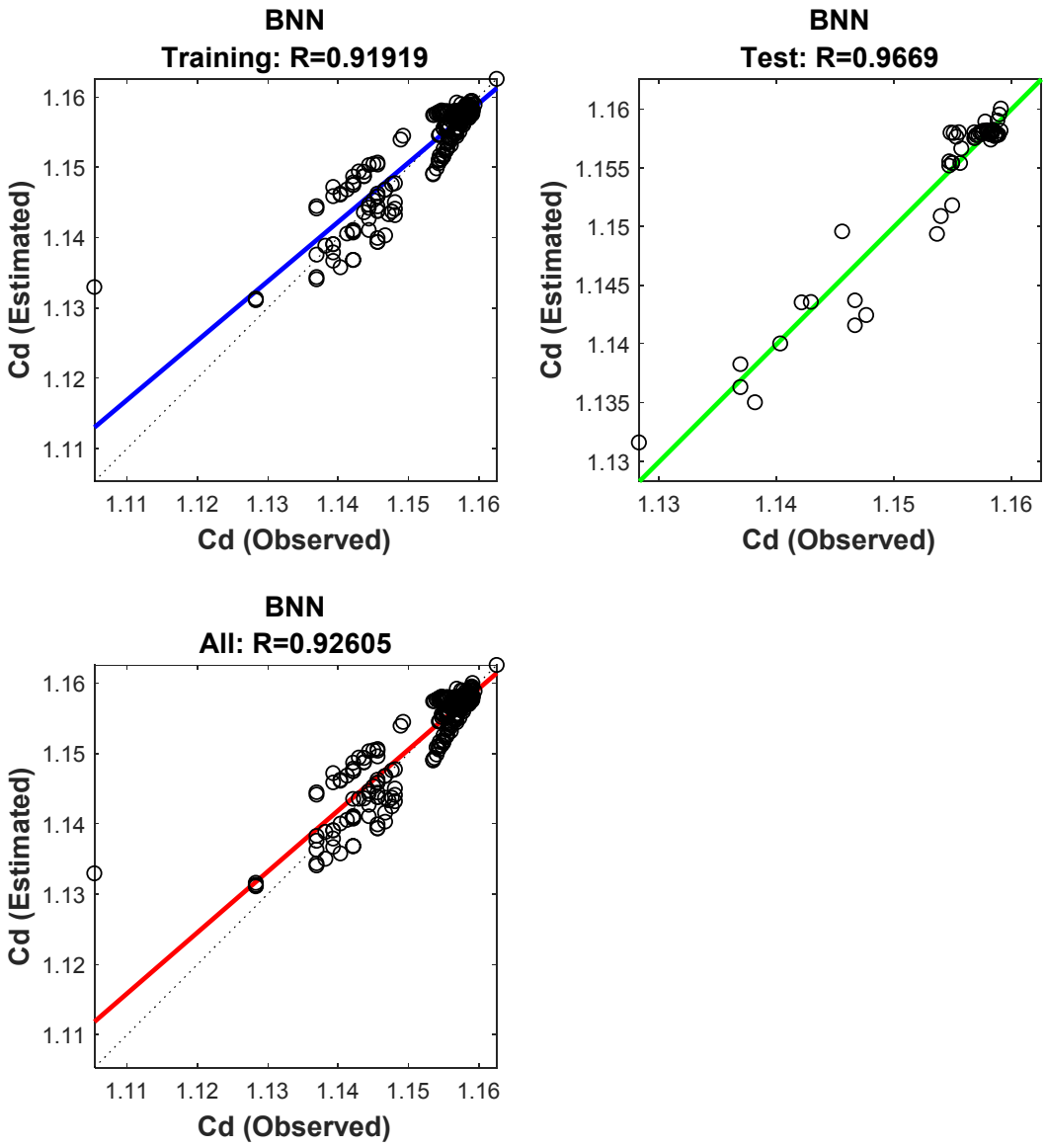

Figure 14: Distribution diagram of the observational-computational values in training and testing stages of Bayesian Neural Network (BNN) Model varification of Cd.

Corresponding author: Yakubu, S. K. ✉ *Khalees2k1@gmail.com* ✉ *Department of Water Resources and Environmental Engineering Ahmadu Bello University, Zaria.*

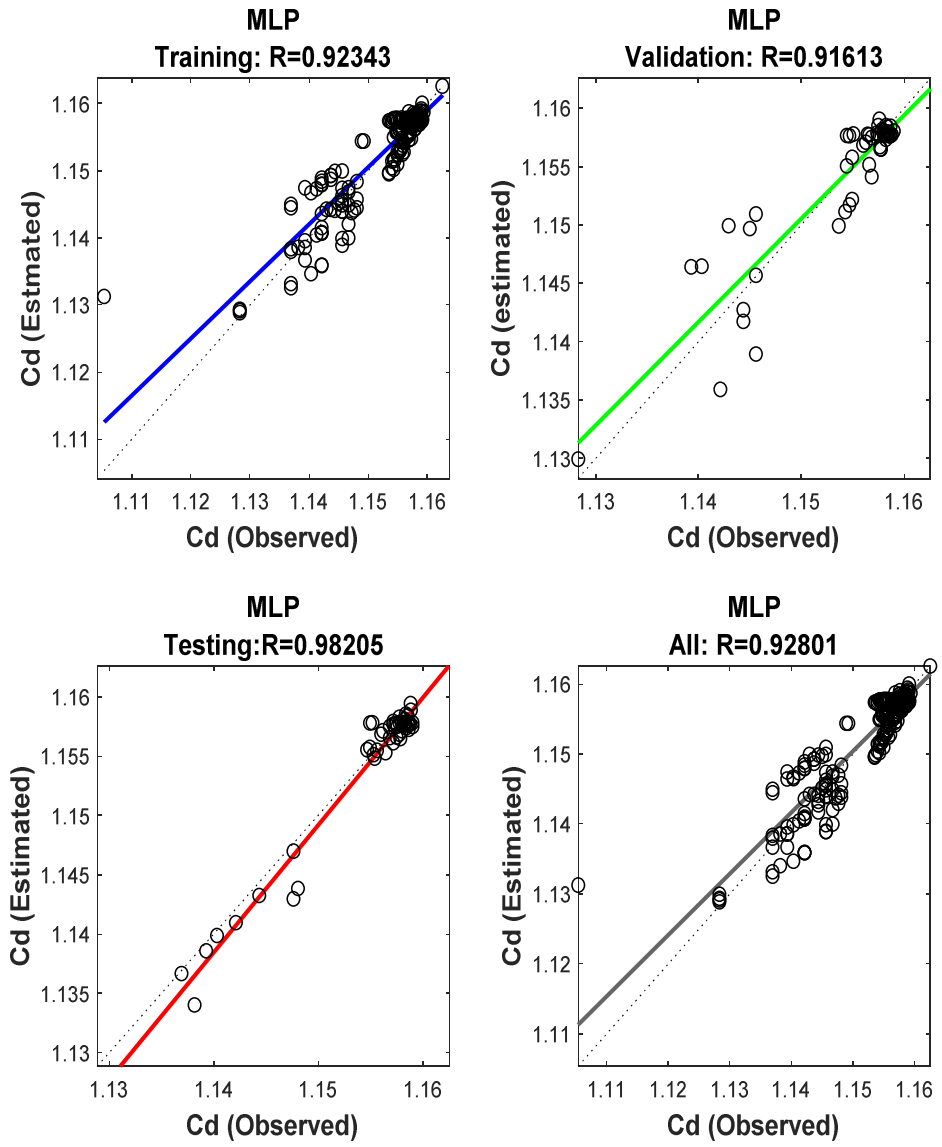

Figure 15: Distribution diagram of the observational-computational values in training and testing stages of MLP model

Thus, the parameters K_1, K_2, a and b in Equation (10) were determined through regression analysis and Curve Fitting Neural Network as expressed by Equation (15) as follows:

$$Cd = 0.5785\left[\frac{D_{50}\theta}{P}\right]^{6.593\times10^{-5}} + 0.58\left[\frac{h}{P}\right]^{0.006761} \quad (15)$$

The model equation has $R^2 = 0.9981$.

Corresponding author: Yakubu, S. K. ✉ *Khalees2k1@gmail.com* ✉ *Department of Water Resources and Environmental Engineering Ahmadu Bello University, Zaria.*

JOURNAL OF SCIENCE TECHNOLOGY AND EDUCATION 9(4), DECEMBER, 2021
ISSN: 2277-0011; Journal homepage: www.atbuftejoste.com

Table 7. Sensitivity analysis of Cd's for input parameters with ANN model.

Function	Training MSE ×(10^{-4})	Training R^2	Testing MSE ×(10^{-4})	Testing R^2
$Cd = \left[\frac{D_{50}\theta}{P}\right]$	7.5421	0.9782	7.6801	0.9884
$Cd = \left[\frac{h}{P}\right]$	3.7313	0.9841	3.8513	0.9971
$Cd = \left(\frac{D_{50}}{P}\theta, \frac{h}{P}\right)$	0.1534	0.9883	0.1635	0.9981

Table 7 shows the sensitivity analysis of Coefficient of discharge, Cd. The sensitivity analysis was carried, in order to evaluate the significance of input variables on the Coefficient of discharge. The sensitivity analysis was performed using the ANN model due to the high value of correlation coefficient and minimum error it produced. Consequently, the parameter ($\frac{h}{P}$) was found to be the most effective parameter with R = 0.9971, MSE = 3.8513x10^{-4} on the prediction of Cd. While the function ($\frac{D_{50}\theta}{P}$) was found to be the least effective parameter on the prediction of Cd.

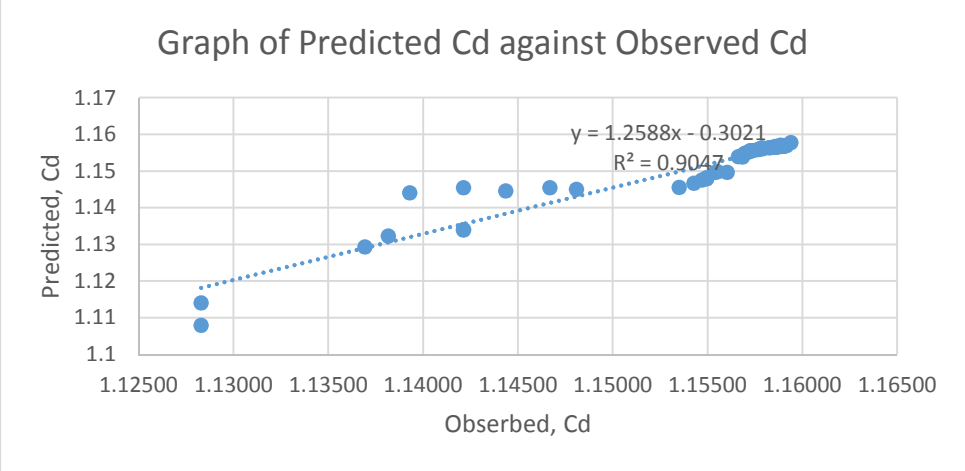

Figure 16: Relation of predicted Cd and observed Cd using (MLP) model

CONCLUSION

By using the equations which has been discussed in the literature, the raw data was calculated and processed using ANN.

Based on the results of the investigation, the following conclusions are reached:

1. Cd increases with the increasing flow rate.
2. The effect of h/P on Cd values increases with the increase in weir height. .
3. The effect of increase of surface roughness on h values will be more on small heights of the crump weir than large ones.
4. C_d decreases from model 1 to model 18 with model 17 having the least C_d close to unity and least percentage error making model 17 to be more efficient.
5. Cd is dependent on the upstream angle, apex angle and downstream angle of the weir. As the upstream angle decreases from 85° to 10°, apex angle increases from 80° to 130° and downstream angle increases from 15° to 40° the Cd is decreasing.
6. The Mathematical Model equation generated using CFNN performed better than other models such as MLP, BNN, GA, MLR, RBF and SVM with

Corresponding author: Yakubu, S. K. ✉ *Khalees2k1@gmail.com* ✉ *Department of Water Resources and Environmental Engineering Ahmadu Bello University, Zaria.*

RMSE= 0.1635×10^{-6}
MAE=0.4713×10^{-3} R^2 =0.9981

7. The model was optimised using GA and the predicted Cd value was 1.14815 as best fitted value.

RECOMMENDATIONS

The recommendations below are some of the improvements that can be carried out for further study:

1. Depth of weir and width of channel in variable value are suggested to get the best flow rate for hydraulic structure of crump weir design.
2. Calibration device for better data collection suggested using a volume meter to get the flow rate over a crump weir.
3. Similar study should be carried out using stones and cement models instead of wooden models.

REFERENCES:

Alauddin, M., Hossain, M., Uddin, M., and Haque, M. (2017). "A Review on Hydraulic and Morphological Characteristics in River Channels Due to Spurs", *World Academy of Science, Engineering and Technology International Journal of Geological and Environmental Engineering*, Vol. 11, No. 4, 397–404.

Al-Naely, H., Al-Khafaji, Z., & Khassaf, S. (2018). Effect of Opening Holes on the Hydraulic Performance for Crump Weir. *International Journal of Engineering, 31*(12), 2022-2027.

Al-Sudani, Z. A., Salih, S. Q., & Yaseen, Z. M. (2019). Development of multivariate adaptive regression spline integrated with differential evolution model for streamflow simulation. *Journal of Hydrology, 573*, 1-12.

Arora K. R. (2005). *Fluid mechanics and hydraulic machines.* Standard publishers Distributors, 1705-B Nai Sarak, Post Box No.: 1066, Delhi-110006.

Azimi H, Bonakdari H, Ebtehaj I (2019) Design of radial basis function- based support vector regression in predicting the discharge coefficient of a side weir in a trapezoidal channel. *Appl Water Sci 9*(4):78

Barr, J., (1910). *Experiments upon the flow of water over triangular notches*. Engineering (London)

Bengtson Harlan (2010). *Open channel flow measurement*. Bright hub. Retrieved March 6, 2011, from http://www.brighthub.com/engineering/civil/articles/65701.aspx

Bos, M.G. (1989). *Discharge measurement structures.* International Institute for Land Reclamation and Improvement (ILRI), publication 20, Wageningen, The Netherlands.

Chanson, H. (2004). *The hydraulics of open channel flow: an introduction*. Butterworth-Heinemann, Oxford, UK, 2nd edition. Retrieved March 6, 2011, from http://www.wikipedia.com

Daneshfaraz R, Minaei O, Abraham J, Dadashi S, Ghaderi A (2019) 3-D Numerical simulation of water flow over a broad-crested weir with openings. ISH J Hydraul Eng. https ://doi.org/10.1080/09715 010.2019.15810 98

Dolcetti, G., & García Nava, H. (2019). Wavelet spectral analysis of the free surface of turbulent flows. *Journal of Hydraulic Research, 57*(2), 211-226.

Ghorbani, M. A., & DEHGHANI, R. (2017). Comparison of Bayesian neural networks and artificial neural network to estimate suspended sediments in the rivers (case study: Simineh rood).

Greve, F. V. (1932). *Flow of water through circular, parabolic and triangular vertical notch weirs.* Purdue Univ. Eng. Bull., 16, No. 2, Res. Series 40

Haghiabi, A. H., Parsaie, A., & Ememgholizadeh, S. (2018). Prediction of discharge coefficient of triangular labyrinth weirs using Adaptive Neuro Fuzzy Inference System. *Alexandria Engineering Journal, 57*(3), 1773-1782.

Heidari, E., Sobati, M. A., & Movahedirad, S. (2016). Accurate prediction of nanofluid

Corresponding author: Yakubu, S. K. ✉ *Khalees2k1@gmail.com* ✉ *Department of Water Resources and Environmental Engineering Ahmadu Bello University, Zaria.*

viscosity using a multilayer perceptron artificial neural network (MLP-ANN). *Chemometrics and intelligent laboratory systems, 155*, 73-85.

Herschy R. W. (1978), *Hydrometry principles and practices.* Department of the Environment Water Data Unit; Reading, A Wiley – Interscience Publication, John Wiley and Sons

Hertzler, R. A. (1938). *Determination of a formular for the 120^0 V-notch weir*. Civil Engineering, 756.

Jan Chyan-Deng, Chia-Jung Chang, and Feng-Hao Kuo (2009), Experiments on Discharge Equations of Compound Broad-Crested Weirs. *Journal of Irrigation and Drainage Engineering © Asce / July/August 2009 / 511*

Jan Chyan-Deng, Chia-Jung Chang, and Ming-His Lee (2006), Discussion of Design and calibration of compound sharp-crested weir by J. Martinez et al. *Journal of Hydraulic Engineering, 132(8), 868–871.*

Karami, H., Karimi, S., Bonakdari, H., & Shamshirband, S. (2018). Predicting discharge coefficient of triangular labyrinth weir using extreme learning machine, artificial neural network and genetic programming. *Neural Computing and Applications, 29*(11), 983-989.

King, H. W. (1916). *Flow of water over right-angled V-notch weir.* Univ. Mich. Technic. 29, No. 3, 189

Khalifa, S. Y., & Umar, A. (2018). Evaluation of Unsteady Open Channel Flow Characteristics over Crump Weir. *ATBU Journal of Science, Technology and Education, 6*(4), 306-315.

Lenz, A. T., (1943). *Viscosity and surface tension effects in V-notch weir coefficients.* Trans. A.S.C.E., 108

Martinez J., Reca J., Morillas M. T., and López J. G.; (2005), Discussion of Design and Calibration of a Compound Sharp-Crested Weir. *Journal of Hydraulic Engineering © ASCE Vol. 131, No.2, pp. 112-116.*

Mehr, A. D., Nourani, V., Kahya, E., Hrnjica, B., Sattar, A. M., & Yaseen, Z. M. (2018). Genetic programming in water resources engineering: A state-of-the-art review. *Journal of Hydrology, 566*, 643-667.

Moazamnia M, Hassanzadeh Y, Nadiri AA, Khatibi R, Sadeghfam S (2019) Formulating a strategy to combine artificial intelligence models using Bayesian model averaging to study a distressed aquifer with sparse data availability. J Hydrol 571:765–781

Muhammad, M. M., Yusof, K. W., Mustafa, M. R. U., Zakaria, N. A., & Ab Ghani, A. (2018). Prediction models for flow resistance in flexible vegetated channels. *International journal of river basin management, 16*(4), 427-437.

Nadiri AA, Sedghi Z, Khatibi R, Sadeghfam S (2018) Mapping specific vulnerability of multiple confined and unconfined aquifers by using artificial intelligence to learn from multiple DRASTIC frameworks. J Environ Manage 227:415–428

Piratheepan M., Winston N.E.F., and Pathirana K.P.P. (2006), Discharge measurements in open channels using compound sharp-crested weirs. *Journal of the Institution of Engineers, Sri Lanka Vol. xxxx, No. 03, pp.31-38.*

Richard H. French (1985), "Open-Channel Hydraulics." Mc Graw Hill, New York.

Rickard C.,Day R.,Purseglove J., 2003," River Weirs – Good Practice Guide", Environment Agency, Rio House, Waterside Drive, Aztec West, Almondsbury, Bristol, BS32 4UD,.

Roushangar K, Alami MT, Majedi Shiri J, Asl M (2017) Determining discharge coefficient of the labyrinth and arced labyrinth weirs using support vector machine. Hydrol Res 49(3):924–938

Sadeghfam S, Daneshfaraz R, Khatibi R, Minaei O (2019) Experimental studies on scour of supercritical flow jets in upstream of screens and modelling scouring dimensions using artificial

Corresponding author: Yakubu, S. K. ✉ *Khalees2k1@gmail.com* ✉ *Department of Water Resources and Environmental Engineering Ahmadu Bello University, Zaria.*

intelligence to combine multiple models (AIMM). J Hydroinform. https ://doi.org/10.2166/hydro .2019.076

Sanikhani, H., Kisi, O., Maroufpoor, E., & Yaseen, Z. M. (2019). Temperature-based modeling of reference evapotranspiration using several artificial intelligence models: application of different modeling scenarios. *Theoretical and applied climatology, 135*(1-2), 449-462.

Sattar, A. A., Elhakeem, M., Rezaie-Balf, M., Gharabaghi, B., & Bonakdari, H. (2019). Artificial intelligence models for prediction of the aeration efficiency of the stepped weir. *Flow Measurement and Instrumentation, 65*, 78-89.

Shen, J. (1960). *Discharge characteristics of triangular-notch thin-plate weirs.* U.S. Dept. of Interior, Geological Survey, draft for I.S.O.

Simon A. L. (1976). *Practical hydraulics.* John Wiley and Sons, Inc. New York. London. Sydney. Toronto.

Yousif, A. A., Sulaiman, S. O., Diop, L., Ehteram, M., Shahid, S., Al-Ansari, N., & Yaseen, Z. M. (2019). Open channel sluice gate scouring parameters prediction: different scenarios of dimensional and non-dimensional input parameters. *Water, 11*(2), 353.

Zahabi H, Torabi M, Alamatian E, Bahiraei M, Goodarzi M (2018) Effects of geometry and hydraulic characteristics of shallow reservoirs on sediment entrapment. Water 10(12):1725 Zhou Q, Zhou H,

Zhou Q, Yang F, Luo L, Li T (2015) Structural damage detection based on posterior probability support vector machine and Dempster-Shafer evidence theory. Appl Soft Comput 36:368–374

Zounemat-Kermani, M., & Mahdavi-Meymand, A. (2019). Hybrid meta-heuristics artificial intelligence models in simulating discharge passing the piano key weirs. *Journal of Hydrology, 569*, 12-21.

Corresponding author: Yakubu, S. K. ✉ *Khalees2k1@gmail.com* ✉ *Department of Water Resources and Environmental Engineering Ahmadu Bello University, Zaria.*